ELSEVIER

Environmental Modelling & Software 15 (2000) 681–692

Environmental Modelling & Software

www.elsevier.com/locate/envsoft

3-D Multi-scale air pollution modelling using adaptive unstructured meshes

A.S. Tomlin [a,*], S. Ghorai [a], G. Hart [a], M. Berzins [b]

[a] *Department of Fuel and Energy, University of Leeds, Leeds LS2 9JT, UK*
[b] *School of Computer Studies, University of Leeds, Leeds LS2 9JT, UK*

Abstract

High resolution models of air pollution transport and transformation are necessary in order to test possible abatement strategies based on pollution control and to forecast high pollution episodes. Models are especially relevant for secondary pollutants like ozone and nitrogen dioxide which are formed in the atmosphere through nonlinear chemical reactions involving primary pollutant species far from their sources. Often we are trying to resolve the interactions between plumes from point sources such as power stations and regional pollution tides of ozone formed in other European countries. One method of tackling this problem of different scales is with different grid sizes, using highly resolved grids in regions where the structure is very fine. This paper describes the use of 3-D adaptive gridding models for pollution transport and reaction using both a layered and a fully adaptive 3-D tetrahedral approach.

Keywords: Air pollution; Dispersion; Adaptive; Unstructured mesh; Resolution; Multi-scale

1. Introduction

One of the greatest numerical challenges in air pollution modelling is to achieve a high resolution solution without overstretching current computational resources. Such high resolution models are needed in order to make comparisons between models and measured data and to enable accurate forecasting of high pollution events. Achieving resolution is a difficult task when often we are considering large numbers of species and many different scales of source types. An obvious way to tackle this problem is to concentrate the computational grid in regions where we gain accuracy from doing so, and to use a coarse mesh elsewhere, thus reducing the total number of solution nodes. Adaptive gridding techniques have been developed as an attempt to automate the grid refinement process so that a priori decisions need not be made about where to place extra mesh elements. They have been used extensively in other reactive flow problems such as combustion but less so in meteorological and air pollution models. However, it is well known that grid resolution has an effect on solution accuracy for advection problems making air pollution models susceptible to inaccuracies when using coarse meshes. The presence of nonlinear chemical reaction processes in air pollution models means that such inaccuracies can be carried through to secondary pollutant formation, possibly affecting total species budget calculations. In the context of air pollution modelling we are interested in the effects of grid resolution in two main areas: local concentrations, and regional species budgets of reactive pollutants. This paper will aim to address a number of questions related to these two areas in the context of the effect of grid resolution in models describing the transport of chemically reacting species. Section 2 describes the approaches used to achieve a solution to the atmospheric diffusion equation. Section 3 describes the mesh generation and adaption procedures. Section 4 demonstrates the effects of mesh resolution for the layered model using a number of test cases. Section 5 demonstrates the tetrahedral scheme and in Section 6 we present a discussion of the results and some conclusions.

2. Model equations and solution strategy

The atmospheric diffusion equation in three space dimensions is given by:

* Corresponding author. Fax: +44-113-244-0572.
E-mail address: alisont@chem.leeds.ac.uk (A.S. Tomlin).

1364-8152/00/$ - see front matter
PII: S1364-8152(00)00038-4

$$\frac{\partial c_s}{\partial t} = -\frac{\partial (uc_s)}{\partial x} - \frac{\partial (vc_s)}{\partial y} - \frac{\partial (wc_s)}{\partial z} + \frac{\partial}{\partial x}\left(K_x \frac{\partial c_s}{\partial x}\right) + \frac{\partial}{\partial y}\left(K_y \frac{\partial c_s}{\partial y}\right) + \frac{\partial}{\partial z}\left(K_z \frac{\partial c_s}{\partial x}\right) + R_s(c_1, c_2, \ldots, c_q) + E_s - (\kappa_{1s} + \kappa_{2s})c_s \quad (1)$$

where c_s is the concentration of the sth compound, u, v, w are wind velocities, K_x, K_y and K_z turbulent diffusivity coefficients and κ_{1s} and κ_{2s} dry and wet deposition velocities, respectively. E_s describes the distribution of emission sources for the sth compound and R_s is the chemical reaction term which may contain nonlinear terms in c_s. For n chemical species an n-dimensional set of partial differential equations (p.d.e.s) is formed describing the rates of change of species concentration over time and space. Each is coupled through the nonlinear chemical reaction terms.

Two approaches have been adopted in the solution of the equation system. The first is to restrict the solution of Eq. (1) to two dimensions and describe the vertical transport using a parametrised approach similar to that used in the LOTOS model and described by van Loon (1996). This is essentially a 2-D approach using a triangular mesh but with four vertical layers describing the surface, mixing, reservoir and upper layers of the troposphere. The equations are discretised on a triangular unstructured mesh using the finite volume method of SPRINT-2D described in detail in Berzins et al. (1992), Berzins and Ware (1995), Tomlin et al. (1997) and (Hart and Tomlin, 1998), Berzins and Ware (1995) and Tomlin et al. (1997). Although the mixing layer height is diurnally varying, the number of vertical layers remains at four and grid refinement is only possible in the horizontal direction (producing a "Toblerone" type mesh). Operator splitting here is achieved at the level of the solution of the nonlinear equation system resulting from the method of lines, thus reducing splitting errors (Tomlin et al., 1997).

The second approach uses a fully 3-D unstructured mesh based on tetrahedral elements. A cell vertex finite volume scheme has been chosen so that the number of mesh elements and therefore flux calculations can be reduced when compared to a cell centered scheme. The dual mesh is constructed by dividing each tetrahedron into four hexahedra of equal volumes, by connecting the mid-edge points, face centroids and the centroid of the tetrahedron. The flux evaluations are cast into an edge based operation. The advective flux is discretised using a second order upwind scheme with limiter, proposed in Barth and Jesperson (1989). This scheme first performs a linear reconstruction to interpolate data to the control volume faces. Monotonicity principles are enforced to ensure that the reconstructed values are bounded by the values of a cell and its neighbours. To this end, multidimensional limiter functions are used. The diffusive term is discretised using a central differencing scheme. Operator splitting is achieved here using a standard approach so that the chemistry and transport steps are treated separately.

3. Mesh generation and adaption

3.1. The meshes

The choice of an unstructured mesh over a regular Cartesian mesh has been made so that resolution of small scale structures such as those due to a point source can be achieved even in a large domain. There is, however, an overhead resulting from the more complex data structures required for an unstructured mesh, and from the complexity of the description of the numerical scheme. The initial unstructured triangular meshes used in SPRINT-2D are created from a geometry description using the Geompack (Joe and Simpson, 1991) mesh generator. For the tetrahedral mesh a cuboid mesh is first formed and the tetrahedra generated by subdividing the cuboids into six tetrahedral elements. Extra mesh points are placed in the lower regions of the boundary layer. Local refinement of the mesh is then achieved by subdividing the triangles or tetrahedra using data structures to enable efficient mesh adaptation. For triangles, regular subdivision results in four sub-triangles, but this may leave some nodes which are unconnected on the edges of the refinement region. These nodes are removed by "Green" refinement which divides triangles into two. Fig. 1 demonstrates regular and "Green" refinement for the tetrahedral mesh. Green refinement is used on the edges of the adapted region so that hanging nodes are removed and each node is connected in the mesh.

3.2. Adaption criteria

Two methods of adaption criteria have been implemented for comparison. The first calculates a first and second order solution and bases the current spatial error on the difference between the two. The spatial error for the next time-step ($e_{i,j}$) is then predicted using interpolation and compared to a user defined tolerance level. A refinement indicator for the jth triangle is defined by an average scaled error which can be measured over all or over a subset of the p.d.e.s:

$$\mathrm{serr}_j = \sum_{i=1}^{npde} \frac{e_{i,j}(t)}{\frac{\mathrm{atol}_i}{A_j} + \mathrm{rtol}_i c_{i,j}} \quad (2)$$

where serr_j is the averaged scaled error, npde the number of p.d.e.s, $e_{i,j}$ the local error estimate of species i over element j, atol_i the absolute tolerance applied to species i, rtol_i the relative tolerance applied to species i, $c_{i,j}$ the

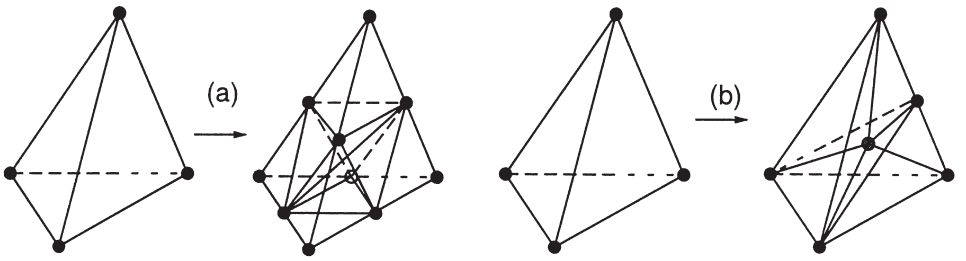

Fig. 1. (a) Regular refinement based on the subdivision of tetrahedra by dissection of interior diagonal (1:8) and (b) "Green" refinement by addition of an interior node (1:6).

concentration of species i over triangle j and A_j the area of the jth triangle. The details of this procedure are more fully explained in Tomlin et al. (1997). The second approach is somewhat simpler and has predominantly been used in the tetrahedral code because of efficiency of calculation. It is based on the calculation of the solution gradient between neighbouring nodes for each species and comparison against a user defined tolerance TOL_g. Refinement is not carried out, however, where low concentrations exist, i.e. lower than the user defined tolerance TOL_c. Both techniques show similar refinement behaviour and adapt in regions of steep spatial gradients. For reactive problems we are interested in a number of species and a user decision has to be made about which species or group of species to refine around. Tolerance values can be set by the user for a single species or a group of species. The results shown here use scaled errors/gradients in total NO_x (i.e. $NO+NO_2$) as the criteria and this seems to give good resolution of structures such as plume characteristics. To some extent, however, the choice of tolerance values will depend on the required output of the model. For advection dominated problems it is necessary to use a safety layer of refinement which means adapting not only for those mesh points where tolerance values are exceeded, but also for directly neighbouring elements or nodes. This point will be illustrated in Section 5.1.

Following adaption, interpolation of solution values onto the new mesh has to be performed. For the cell centred triangular scheme this is performed using the Ramshaw "rezoning" method which is first order but preserves mass balance. For the tetrahedral scheme the process is more complex because it is cell vertex based. Concentration values have to be interpolated to the new nodes (refinement) or redistributed from the deleted nodes to the existing neighbouring nodes (derefinement), ensuring that the total mass remains the same and interpolation errors are small. The cell-vertex method uses cell-centred dual volume elements to enforce mass conservation. The main features of the method are as follows:

(i) Prior to adaption the mass in every element is calculated from the contribution of nodes forming the element.
(ii) Post adaption the concentrations in the child nodes are estimated by linear interpolation.
(iii) The mass in each of the child elements is calculated from the concentration of the nodes forming the elements.
(iv) This mass is scaled so that the total mass in the child cells is equal to the mass in the parent cell.
(v) The mass contribution to the new nodes is calculated from the adjacent elements and is divided by the control volume to form the concentrations on the new mesh.

The errors induced by the interpolation procedure are small, as demonstrated in Section 5.1 where predictions from the method are compared to an analytical solution of a test problem.

3.3. Interpolation of wind data

Another issue which arises when using unstructured adaptive meshes is the need to interpolate physical data onto refined mesh structures. One example is the interpolation of non constant wind data which is often obtained either from synoptic data or from meteorological models based on structured meshes. Again this interpolation has to be carried out in a conservative way whilst causing minimal changes in wind velocities. This is achieved using the variational calculus method of Mathur and Peters (1989). Space does not allow details to be given here but the method can be summarised as allowing minimal changes to be made to the interpolated data in the least squares sense whilst satisfying the mass conservation constraint using minimisation of a cost functional. Initial tests have shown that the interpolation technique can lead to adjustments in the wind field of a few cm s^{-1} for horizontal components and a few mm s^{-1} for vertical components for adapted meshes. The velocity corrections are therefore small in comparison to standard wind velocities and are not thought to be of concern, since any errors induced are greatly outweighed by the gains in accuracy made by the increased resolution of the mesh.

4. Test cases

The following test cases have been designed to investigate the effects of mesh resolution on the solution of Eq. (1) for situations representative of those in regional scale air pollution models.

4.1. The effects of horizontal refinement for the layered mesh

As emissions inventories improve it will become common to represent data as point, line and area sources on a regional basis. It is therefore important to investigate the effects of mesh resolution on the representation of transport and reaction from various source types. The following results show the effect of resolution for the transport and reaction from a single NO_x source through a background of volatile organic compounds (VOCs) and ozone.

4.1.1. Passive dispersion

If we first neglect chemical reaction terms we see the effect of the mesh on turbulent transport. The results shown below represent the dispersion in a single westerly wind direction at 6 m s^{-1} from a point source of NO_x of 400 kg h^{-1} at a height of 330 m. Fig. 2(a) and (b) show the dual meshes for both the coarse and the refined simulation. The refinement region is seen to be along the plume centre where the concentration gradients are high. Fig. 3 shows the down-wind concentrations of NO for different levels of mesh refinement ranging from approximately 300 m up to 9 km in edge length. The difference in NO concentrations is around a factor of 4 at a distance of 30 km from the source and a factor of 2.5 for the peak concentrations. It should be pointed out here that even the coarsest mesh of 9 km would be considered to a reasonable level of resolution in a regional scale model and that larger meshes would result in even higher errors.

The reason for the high level of error can be attributed to high levels of numerical diffusion from the coarse mesh. A simple calculation based on the determination of plume width for different meshes and a Gaussian approach demonstrates that the numerical diffusion for the coarsest mesh is in fact eight times that represented by K_x and K_y. The conclusion from this simple test case must be that the types of meshes commonly used in regional and larger scale dispersion models seriously overestimate the levels of mixing from concentrated sources, and therefore underestimate down-wind concentrations. In fact in most cases the amount of numerical diffusion is probably greater than that represented by K_x and K_y. The effects of numerical diffusion are especially exaggerated for point source types because of the resulting steep gradients. For models which include emissions databases capable of representing point and lines sources, model resolution will therefore be an important issue. The limited vertical resolution in the layered model is also an important issue and we will return to this point later.

4.1.2. Reactive plume

The smearing of the concentration profile due to numerical diffusion will have an obvious effect on the chemical reaction rates and this can be demonstrated by studying profiles of secondary species such as NO_2 and O_3 for the same point source as in the previous section. Chemical reaction terms in the model are represented by both the GRS scheme (Venkatram et al., 1994) and a carbon bond type scheme (Heard et al., 1998) for comparison, showing similar local concentration profiles for O_3, but slightly different effects with regards to the mesh. Local concentrations of O_3 and NO_2 are clearly affected by grid resolution for both chemical schemes. Fig. 4(a) and (b) demonstrate this effect for the GRS scheme. For ozone the minimum concentration at the plume core is overestimated by the coarse grid and the peak ozone concentrations shifted outwards. Maximum NO_2 concentrations are underestimated by a factor of 2 for a factor of 4 change in grid resolution. Total species budgets which are calculated by summing concentrations across the domain are also affected by grid resolution. Fig. 5 shows the total ozone concentration in the surface layer for the whole domain over 1 day of the diurnal cycle using the Carbon Bond scheme. Here the peak ozone concentration around mid-day is overestimated by the coarser grid. The effects are much less pronounced for the GRS scheme, which is perhaps not surprising since it uses a very simple description of the nonlinear processes involved in ozone generation. The effects of grid resolution on secondary pollution prediction therefore seem to be chemical scheme dependent.

4.1.3. Regional scale model

The results from the single source test clearly demonstrate the effects of mesh resolution on secondary species predictions. Regional scale comparisons have also been made using the same layered approach and multi-scale emissions data. A European scale model is used in order to establish boundary conditions for the regional scale model which covers a large part of the UK. EMEP emissions data for 1994 is used on the European scale giving information about NOx and VOC emissions on a 50×50 km grid for most of Europe and a 150×150 km for some parts. For the UK, point source and area emissions data (10×10 km) from NETCEN have been used. Area sources are interpolated onto the triangular grid using the Ramshaw method. Point sources are simply averaged into the mesh element where they are contained. It follows therefore that for finer meshes a more concentrated source will be represented. Dry deposition and vertical dispersion are included following the approach of van

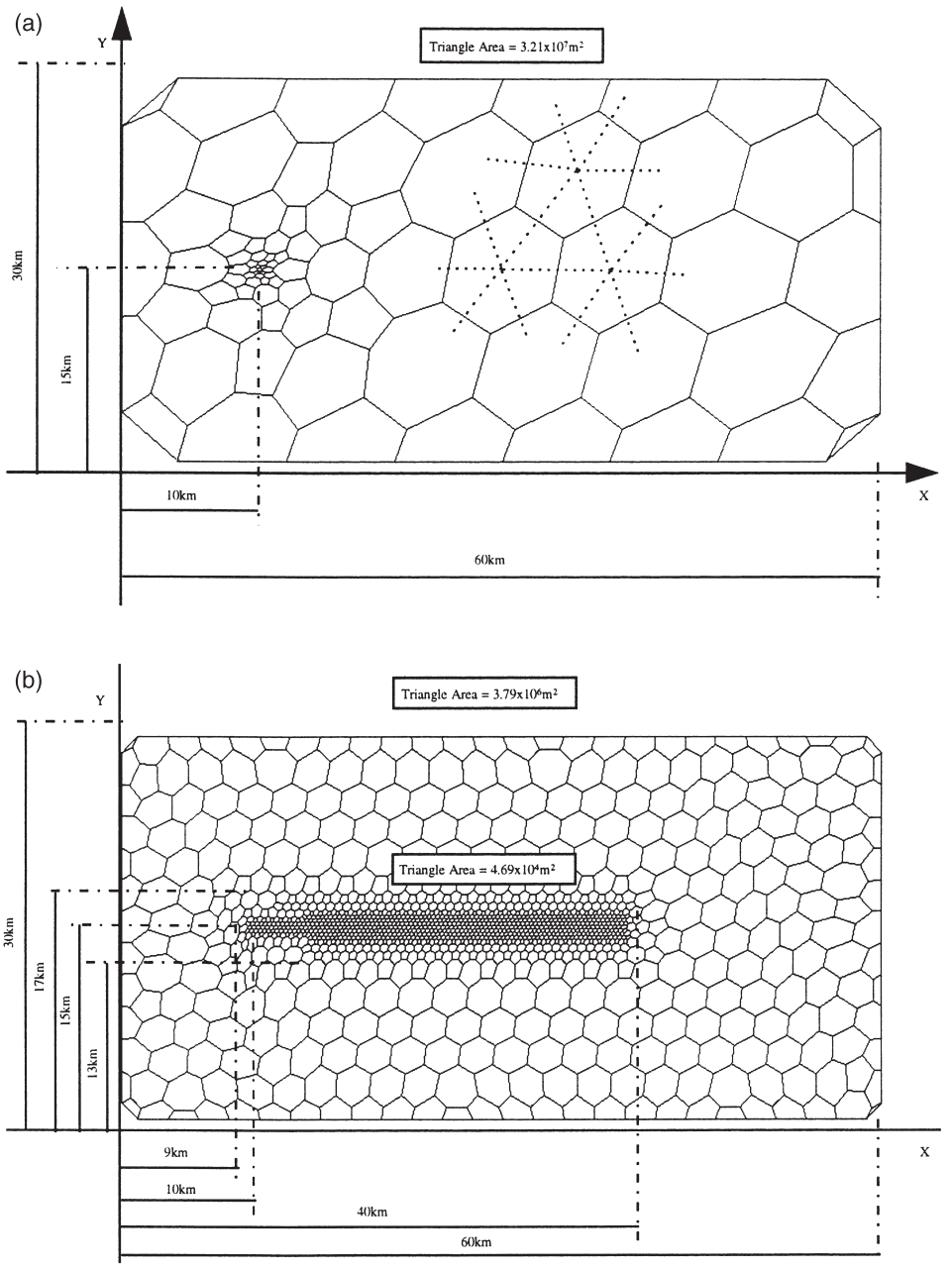

Fig. 2. Dual mesh for passive dispersion from a single NO_x source showing (a) course mesh and (b) adaptive mesh with refinement along the plume centre.

Loon (1996). The meshing technique has been to use a large scale grid over Europe in order to provide boundary conditions for the regional scale model. A nested region with some refinement has been defined over the UK and transient refinement to finer meshes is allowed in this region according to the spatial error of the solution. A maximum refinement level has to be provided by the user since point sources will otherwise reach high gradients leading to further refinement requirements. Usually there are about five levels of refinement from the European to the local scale with mesh elements ranging from 150 to 2 km in terms of edge length. Wind data has been interpolated onto the mesh from synoptic station data.

Space does not permit a detailed discussion of the effects of mesh resolution for the regional scale model, but some preliminary results will be presented here which demonstrate similar effects to the simple test case. Refinement generally takes place in regions with high spatial gradients such as along the edges of power stations and urban plumes. In order to represent these interactions significant refinement is sometimes necessary, as shown in Fig. 6. This mesh was generated during a simulation of an ozone episode which took place at the

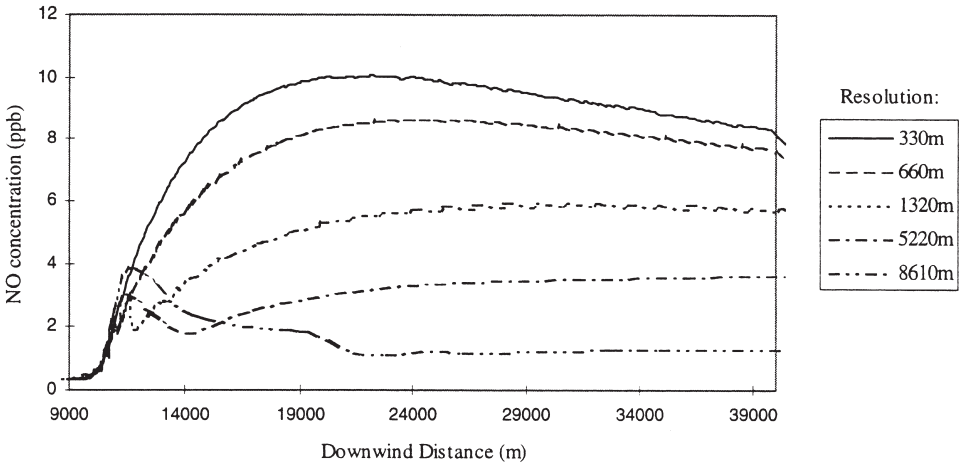

Fig. 3. Down-wind concentration of NO for passive plume for varying mesh resolutions.

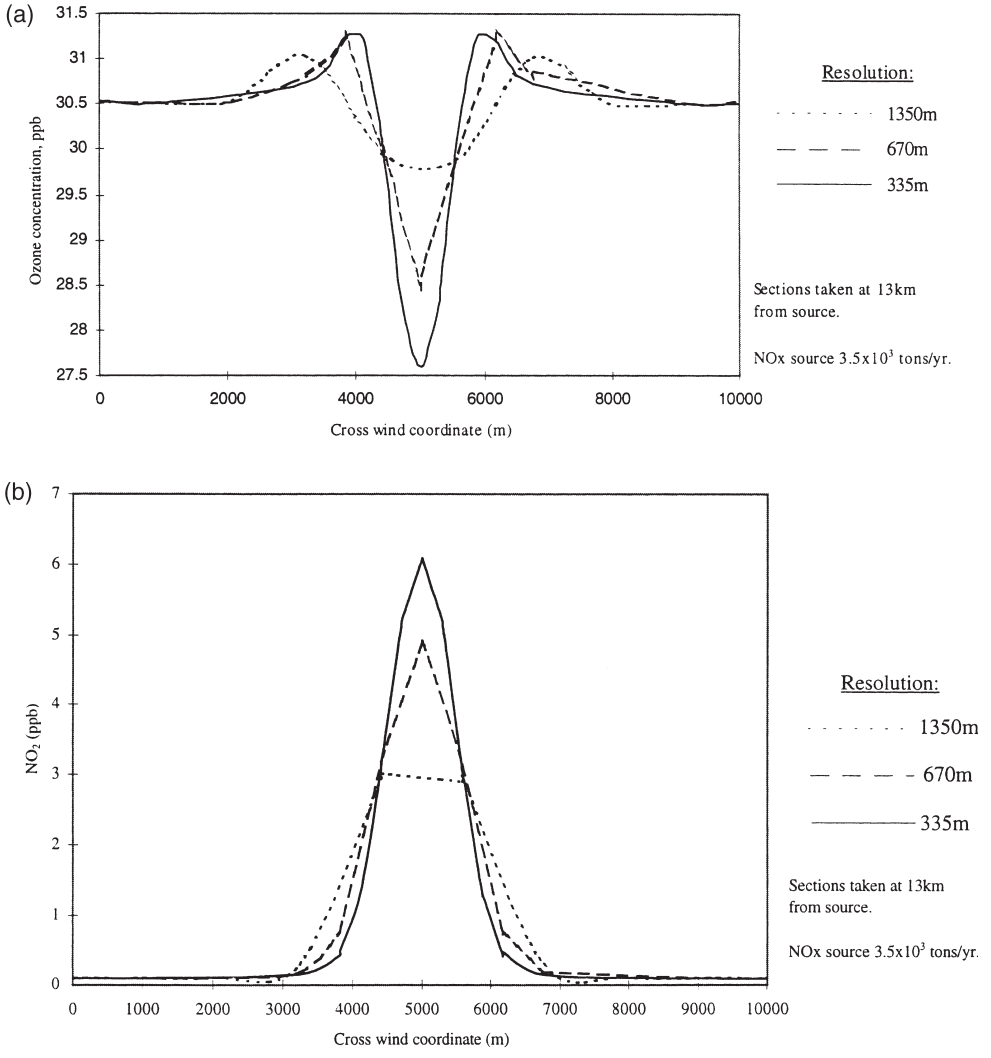

Fig. 4. Plume profiles of (a) ozone and (b) NO_2 for varying mesh resolutions.

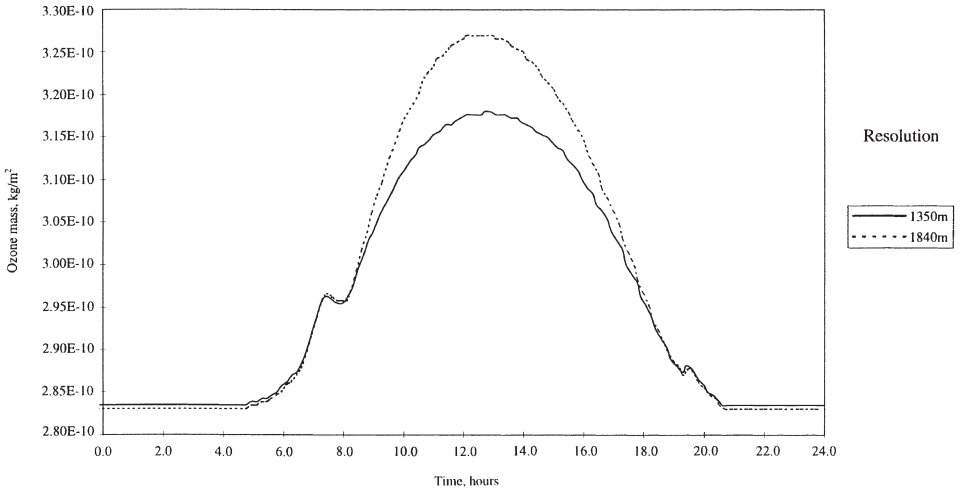

Fig. 5. Total ozone concentration in the surface layer for the whole domain showing the effects of mesh resolution on total species budgets.

beginning of July 1994 and this particular set of conditions is a result of winds from the west of the UK. The refinement region therefore follows plumes towards the east. The base mesh within the UK region is of edge length 28 km with refinement a further three levels to 3.5 km.

Fig. 7 shows the total species mass of O_3 and NO_2 in the surface layer, calculated using the GRS scheme over 2 days of simulation for the base and the level 3 refined mesh. Resolution clearly affects the species budget of NO_2 showing about a 20% difference in peak masses. Ozone is less sensitive to mesh resolution as far as total budgets are concerned. There is some small effect on minimum concentrations, but very little on maxima. An explanation for this may be that most ozone is generated away from source regions where concentration gradients are less steep and that the GRS scheme is not highly non-linear in terms of O_3. Further refinement below level 3, i.e. to mesh sizes below about 3 km, does not seem to have a significant effect on the total species budgets, even for NO_2. This suggests that if the aim of a model is to estimate general ozone or NO_2 trends over large time-periods a courser mesh would be suitable. Refinement to fine meshes leads to stability problems due to the CFL condition and consequently smaller time-steps. Long-time period calculations would then become quite expensive and the cost of achieving high resolution would outweigh accuracy gains.

For local forecasts and comparison with monitored data, refined meshes are more important, particularly in areas where many sources of different scales are present. Fig. 8 shows profiles taken across the mesh from south to north for O_3 and NO_2 for the base and level 3 mesh at 3.00 pm on 1 July, where the maximum ozone concentrations occur. Here the effects of the mesh are more apparent than for total species budgets with peak concentrations being underpredicted by the coarse mesh by almost a factor of 2 for O_3 and a factor of 3 for NO_2. Most of the structure which is generated by plumes is lost by the coarse mesh. This suggests that validation of a coarse mesh model by comparison with monitored data such as that obtained from flight measurements could lead to an underestimation of peak concentrations.

5. Vertical refinement using tetrahedral meshes

The layered model uses a highly parametrised description of mixing in the vertical direction. This will have a large effect on near source concentrations as enhanced mixing caused by coarse layering will change the vertical profile of a plume. A tetrahedral model has therefore been developed which can adapt in the vertical plane, allowing improved vertical grid resolution. First the advection scheme has been tested using a standard rotation problem.

5.1. Molenkampf test

To verify the advection scheme using a limiter, we used the linear advection equation of Molenkampf (1968). The dimensions of the base grid in the horizontal, lateral and vertical directions are 60 km, 15 km and 3 km, respectively. The initial conditions can be described as a sphere with centre at $(x_0, y_0, z_0)=(30, 3, 0.3)$ km,

$$c(x, y, z)=10^{11}\exp(-\kappa[(x-x_0)^2+(y-y_0)^2+100(z-z_0)^2])$$

where c is in molecules cm^{-3} and $\kappa=7.5\times10^{-11}$. The test equation is

$$\frac{\partial c}{\partial t}+(y-y_1)\omega\frac{\partial c}{\partial x}+(x_1-x)\omega\frac{\partial c}{\partial y}=0$$

where $\omega=10^{-4}$ and $(x_1, y_1) = (30, 7.5)$ km. The period of the rotation is approximately 17.44 h. The grid is refined

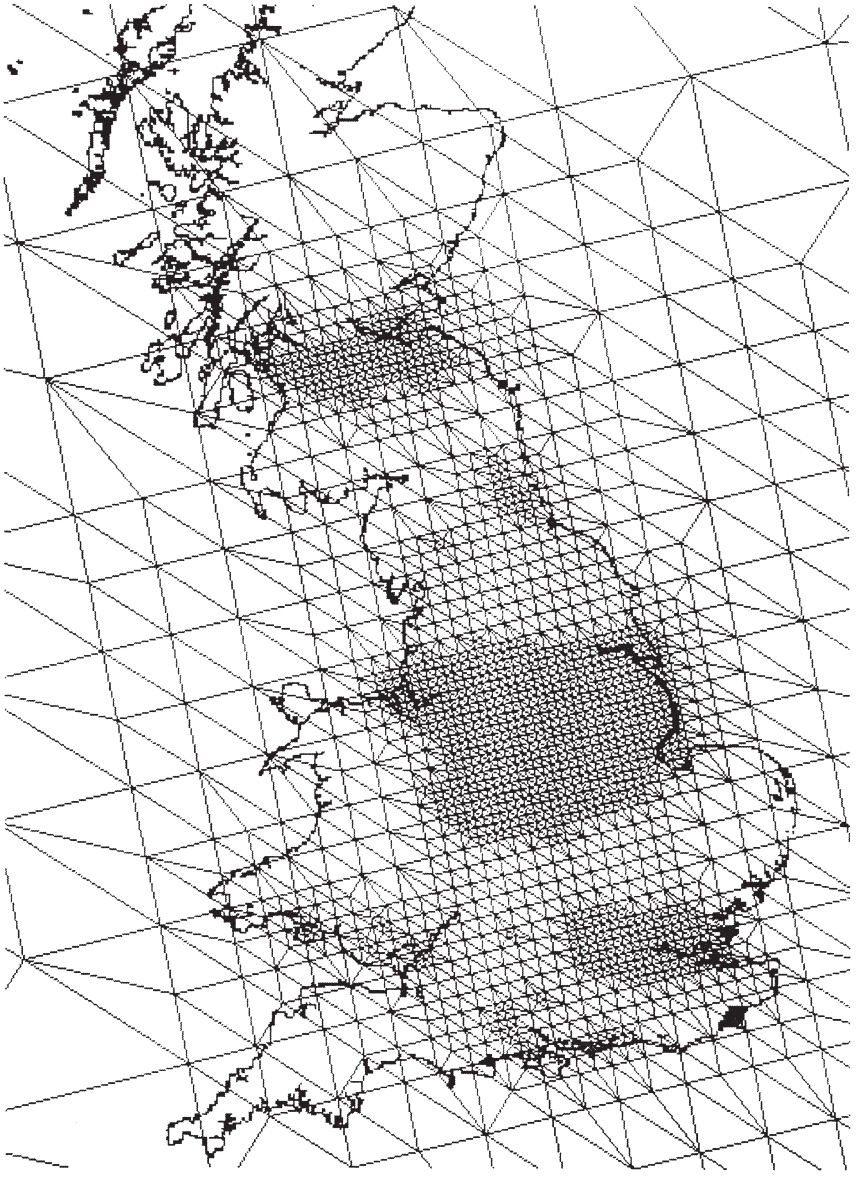

Fig. 6. Typical mesh used in the refinment region for UK.

by three levels if the concentration gradient and concentration values exceed some tolerance parameters. The initial grid consists of 4961 tetrahedra and the final grid after approximately one rotation contains 11,638 tetrahedra.

Fig. 9 shows the peak concentrations at t=0 and after one rotation of the sphere. The final peak is about 91% of the original, showing that little numerical diffusion is taking place. The Molenkampf problem demonstrates the importance of using a safety layer around the high resolution region. The advantage of this is that as the region of steep gradients advances due to advection, the cells ahead of the front are already of high resolution and the plume front is not diluted into large cells. Without the safety layer steep gradients may be advected into a large grid cell so that the solution is smeared and the gradient drops. Further refinement will then be prevented. This implies that the best strategy to start a model with multiple source points and a complex initial concentration field would be to use a refined mesh and then coarsen the mesh where the gradients are low. In this way it will be certain that initial steep gradients are maintained throughout the simulation.

A small amount of vertical numerical diffusion resulting from a horizontal advection scheme is a side effect of using fully unstructured meshes. As Cartesian meshes are usually aligned to the surface we would not expect them to demonstrate this problem for modelling dispersion over flat terrain. However, the results show that the total overall diffusion is kept small if sensible mesh refinement is used.

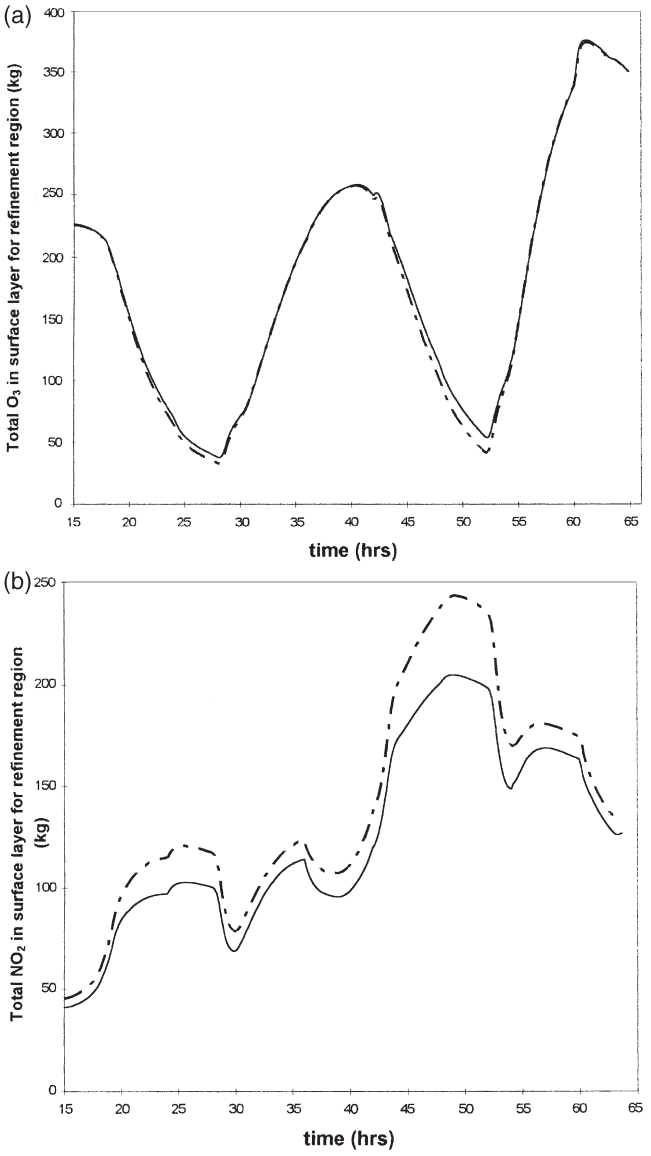

Fig. 7. Total species budgets for 2 days of simulation during a July episode in 1994. Mass has been summed over the refinement region which covers much of the UK. The bold line represents three levels of refinement over the base mesh represented by the dashed line. (a) Total ozone mass in the surfaced layer; (b) NO_2 mass in the surface layer.

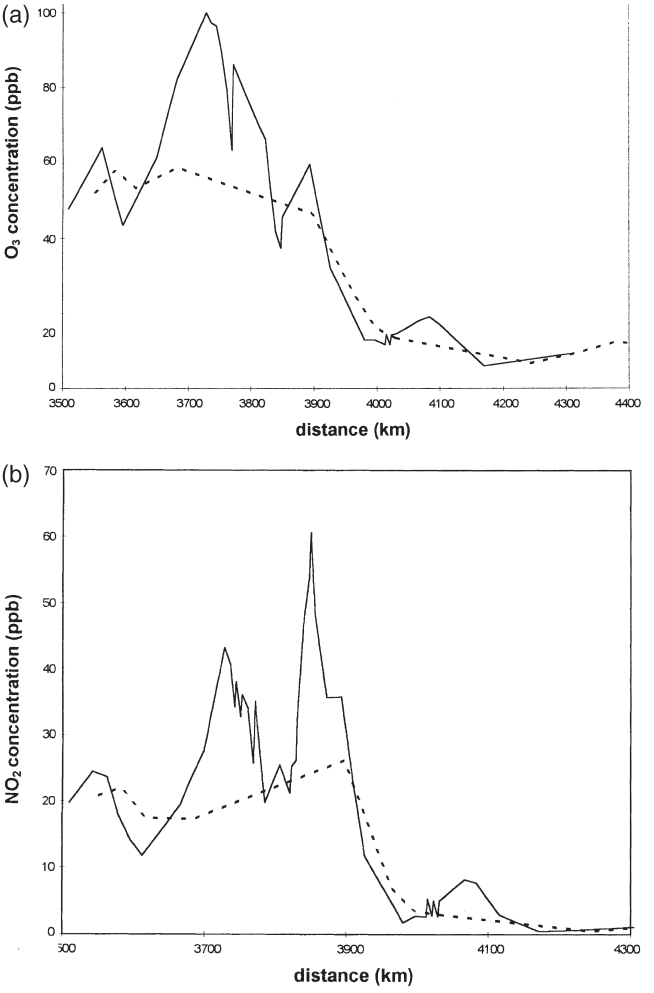

Fig. 8. Example cross mesh profiles for (a) O_3 and (b) NO_2 for 3 pm on 1 July 1994. The bold line represents three levels of refinement over the base mesh represented by the dashed line.

5.2. Comparison of CPU requirements for advection diffusion case

Here we investigate the usefulness of the adaptive gridding technique compared to fixed mesh approaches. The test consists of advecting a puff of NO around a horizontal circle as in the previous section, although in this case with diffusion. The peak of the puff therefore decreases as it is carried around the circle. The background concentration is 2.5×10^9 molecules cm^{-3}. The dimensions of the domain are 80 km, 60 km and 3 km, respectively. We define a sphere at (x, y, z)=(30, 30, 0.23) km such that the background NO concentration is 2.5% of the value of NO at the centre of the sphere. The value of the concentration away from the centre approaches the background value exponentially. The wind velocities are chosen such that the period of rotation is 24 h. We chose K_x=K_y=50 m^2 s^{-1} for the horizontal diffusion parameters. The vertical diffusion profile is one typical of a neutral boundary layer model and is shown in Fig. 10.

The number of nodes in the base mesh is 3696, which is produced by dividing the domain into 20×15×10 cuboids. A new mesh is then defined by refining all the edges to level 3 whose connected nodes lie within 10 km horizontally from the circumference of the path of the sphere and 1 km from the ground level. The number of nodes in this new grid is 191,616 and is equivalent to a fully refined mesh, therefore providing a reference solution. We now compare the adaptive solution with refinement to level 3 with a "telescopic" solution where the grid is refined to level 3 around the initial peak, but no further refinement takes place. Fig. 11 presents a

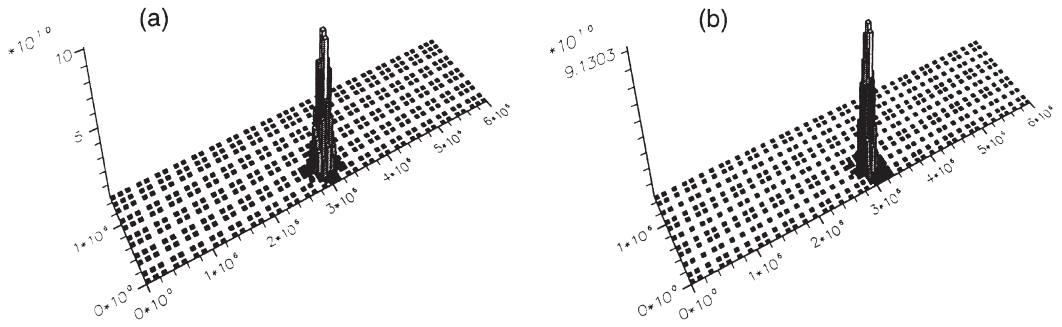

Fig. 9. Molenkampf problem for tetrahedral mesh, (a) Initial concentration of peak and (b) peak concentration after one rotation.

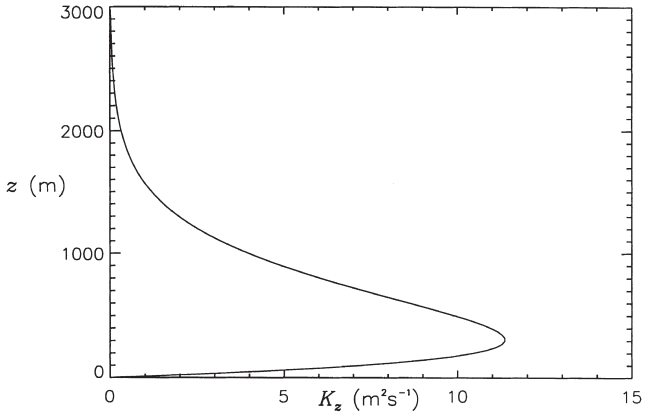

Fig. 10. Vertical diffusion profile used in test case 5.2.

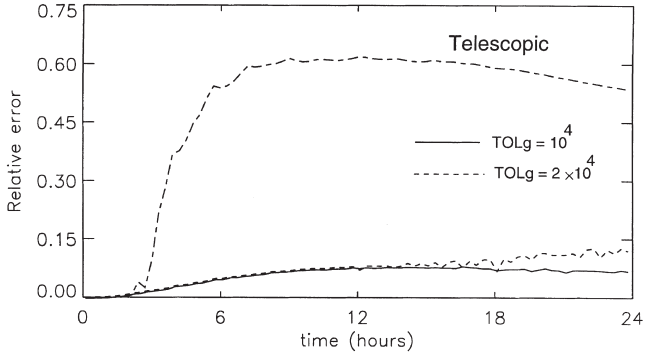

Fig. 11. Comparison of relative errors of adaptive and telescopic methods when compared to reference solution for test case 5.2.

comparison of the relative error when compared to the reference solution for two adaptive cases with slightly different tolerances, and the telescopic solution. The results demonstrate that the adaptive solution remains within 10–15% of the reference solution, depending on the chosen tolerances and that the telescopic method is very unreliable. The choice of tolerance and therefore accuracy will obviously affect the number of refined nodes and therefore solution time. Table 1 summarises the properties of the mesh and total CPU time required for solution. The adaptive solution is approximately three times slower than the unrefined solution but with a significant gain in accuracy. It is approximately six times faster than the reference calculation, even for the tighter tolerance values.

5.3. The effect of mesh resolution on vertical profiles

The possibility of refinement in the vertical direction should improve near source predictions over the layered mesh, although it is acknowledged that using a simple diffusion model plume intermittency cannot be represented. The effects of mesh resolution for a single passive source will now be demonstrated for the same NO_x source as in Section 4.1.1. The value of K_z is 20 $m^2\ s^{-1}$ and although a direct comparison of vertical diffusion levels cannot be made for both approaches both sets of results correspond qualitatively to neutral conditions. The base mesh consists of elements of length 4 km in the horizontal directions and has 10 vertical layers up to 3 km. Refinement to three levels has been maintained around the source in order to prevent immediate diffusion. Fig. 12(a) shows the ground level down-wind profiles for various levels of mesh refinement. Comparison with Fig. 3 shows that although the peak concentrations are similar for the refined meshes the qualitative profile is somewhat different to that obtained using the layered mesh in that the concentration falls off to much lower levels. The effect of mesh resolution is quite pronounced for the peak ground level concentrations close to the source, but less important at large distances downwind where the gradients are smoother and the refinement less. Fig. 12(b) shows a vertical profile taken along the plume core at a distance of 16 km from the source. Here the effects of resolution can be seen quite clearly to affect the peak concentrations. The larger meshes show a much smoother vertical profile than the adapted mesh.

Table 1
Comparison of adaptive solutions with respect to different fixed grid methods for test case 5.2

Method	TOL_c TOL_g	Initial nodes	Final nodes	Max. nodes (time)	Total CPU time	Max % error
Fixed	– –	191,616	191,616	191,616 (–)	32:15 h	(–)
Telescopic	– –	15,067	15,067	15,067 (–)	1:44 h	60
Adaptive	0.5×peak value 10^4	15,067	22,993	27,708 (18:50 h)	5:27 h	10
Adaptive	0.5×peak value 2×10^4	15,067	15,555	19,773 (18:50 h)	3:51 h	15

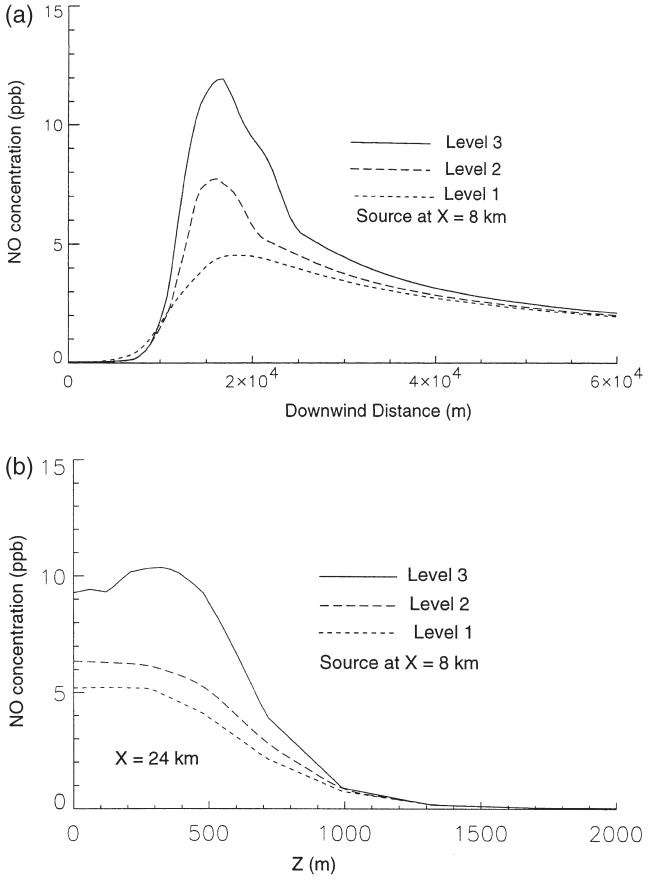

Fig. 12. (a) Down-wind ground level NO concentrations for the tetrahedral mesh and a single NO_x source. (b) Vertical profiles along the core of the plume, 16 km from the source.

6. Discussion and conclusions

The test cases studied clearly demonstrate the need for finer meshes when predicting local concentrations. This point will become even more important as emissions databases develop in their ability to represent different source types. Point sources particularly are immediately smeared when averaged into large grid cells and without transient refinement plume structures cannot be captured. For ozone, total species budgets were not highly mesh sensitive but the same is not true for other species such as nitrogen products. The conclusion may perhaps be that for long-time species budget calculations of ozone a certain amount of adaptivity will be useful, but refinement to very small meshes is not worthwhile because of the computational burden of extra mesh elements and a smaller time-step due to the CFL condition. The sensitivity of the model to mesh resolution was, however, seen to be dependent on the chemical scheme chosen.

The accuracy of the adaptive tetrahedral model was seen to approach that of the reference solution for the test case studied, although requiring much lower computer resources. A comparison of a layered approach with a fully 3-D adaptive approach has shown that vertical mesh resolution is also important in resolving near source vertical profiles. Layered models in fact may be overestimating ground level concentrations at large distances from the source.

References

Barth, T.J., Jesperson, D.C., 1989. The design and application of upwind schemes on unstructured meshes. AIAA-89-0366, 9–12 January.

Berzins, M., Lawson, J., Ware, J., 1992. Spatial and temporal error control in the adaptive solution of systems of conversation laws. In: Vichnevetsky, R., Knight, D., Richter, G. (Eds.), Advances in Computer Methods for Partial Differential Equations VII. IMACS, pp. 60–66.

Berzins, M., Ware, J.M., 1995. Positive cell-centered finite volume discretization methods for hyperbolic equations on irregular meshes. Appl. Num. Math. 16, 417–438.

Heard, A.C., Pilling, M.J., Tomlin, A.S., 1998. Mechanism reduction techniques applied to tropospheric chemistry. Atmos. Env. 32, 1059–1073.

Joe, B., Simpson, R.B., 1991. Triangular meshes for regions of complicated shape. Int. J. Numer. Meth. Eng. 23, 987–997.

Mathur, R., Peters, L.K., 1989. Adjustment of wind fields for application in air pollution modelling. Atmos. Env. 24A, 1095–1106.

Molenkampf, C.R., 1968. Accuracy of finite-difference methods applied to the advection equation. Journal of Applied Meteorology 7, 160–167.

Tomlin, A.S., Berzins, M., Ware, J., Smith, J., Pilling, M.J., 1997.

On the use of adaptive gridding methods for modelling chemical transport from multi-scale sources. Atmos. Env. 31, 2945–2959.

van Loon, M., 1996. Numerical methods in smog prediction. PhD thesis.

Venkatram, A., Karamchandani, P., Pai, P., Goldstein, R., 1994. The development and application of a simplified ozone modelling system (SOMS). Atmos. Env. 27B, 3665–3678.